

To appear in The Astronomical Journal, January 1998 issue

Radial Velocities of Globular Clusters in the Giant Elliptical Galaxy NGC 1399

Dante Minniti^{1,2}, Markus Kissler-Patig^{3,2,4}, Paul Goudfrooij^{5,6,2}, and Georges Meylan²

ABSTRACT

We report on the radial velocity measurements of 18 globular clusters and one dE galaxy in the field of the giant elliptical galaxy NGC 1399, the dominant galaxy of the Fornax cluster. We present also the radial velocity measurements of some candidates for young and super metal-rich globular clusters, which turn out to be foreground or background objects, viz. 28 stars and 7 galaxies. The bona fide globular clusters are selected, on the basis of their magnitudes and colors, to be metal-rich. For this cluster sample we measure a mean radial velocity of $v_{rad} = 1353 \pm 79 \text{ km s}^{-1}$, and a velocity dispersion of $\sigma = 338 \pm 56 \text{ km s}^{-1}$. Using a few different mass estimators, this implies M/L values in the range 50 – 130 within a radius of 28 kpc, consistent with M/L rising with radius. Our velocity dispersion estimate σ is intermediate between the value computed from the integrated stellar light at smaller radii, and that computed at large radii from recent X-ray observations.

Subject headings: Galaxies: individual (NGC 1399) – Galaxies: clusters (Fornax) – Galaxies: dynamics – Galaxies: Dark matter – Globular clusters

¹Lawrence Livermore National Laboratory, Livermore, CA 94550, USA

E-mail: dminniti@llnl.gov

²European Southern Observatory, Karl-Schwarzschild-Str. 2, D-85748 Garching bei München, Germany
E-mail: gmeylan@eso.org

³Lick Observatory, University of California, Santa Cruz, CA 95064, USA
E-mail: mkissler@ucolick.org

⁴Sternwarte der Universität Bonn, Auf dem Hügel 71, D-53121 Bonn, Germany

⁵Space Telescope Science Institute, 3700 San Martin Drive, Baltimore, MD 21218, USA
E-mail: goudfroo@stsci.edu

⁶Affiliated with the Astrophysics Division, Space Science Department, European Space Agency, ESTEC, Postbus 299, NL-2200 AG Noordwijk, The Netherlands

1. Introduction

A globular cluster contains about 10^5 stars of different masses, generally with similar ages and metallicities. From both dynamical and stellar population points of view, globular clusters appear significantly simpler than galaxies. Because they can be observed to much larger distances than individual stars, properties of globular clusters can be used to study the formation and evolution of their host galaxies. In particular, the discovery of a very large number of clusters associated with the giant elliptical galaxy M87 (Baum 1955; Racine 1968; Forte et al. 1981; Strom et al. 1981) generated a number of fascinating questions about the formation of cluster systems of giant elliptical galaxies (e.g., van den Bergh 1990; Ashman & Zepf 1992; Harris 1995; Kissler-Patig 1997; Forbes et al. 1997a).

Particularly interesting is the discovery of bimodality in the color distribution of the globular cluster systems of some elliptical galaxies, which has been generally interpreted as a bimodal metallicity distribution (e.g., Zepf & Ashman 1993; Geisler et al. 1996 Whitmore et al. 1996). This suggests that the globular cluster systems of some ellipticals may be a superposition of different cluster populations.

More progress in the understanding of the formation of cluster systems in galaxies is coming from large radial velocity surveys (e.g., Mould et al. 1987, 1990; Grillmair et al. 1994; Hui et al. 1995; Bridges et al. 1997, Cohen & Ryzhov 1997). Globular cluster systems are ideal probes for studying the dynamics of the outer parts of galaxies, where the surface brightness of the galaxy itself becomes too faint to provide useful kinematic data. Furthermore, the masses of globular clusters are negligible with respect to the mass of the galaxy so that they directly trace the underlying gravitational potential. Radial velocity surveys of globular cluster systems thus provide a powerful means to constrain the dynamical predictions of elliptical galaxy formation scenarios (e.g., isotropy, dark matter content). This is nicely illustrated by the recent work by Cohen & Ryzhov (1997), who are able for the first time to accurately map the radial dependence of M/L in M87, using radial velocities from *Keck* spectroscopy of a large sample of 205 globular clusters.

In this paper we concentrate on the globular cluster system of NGC 1399, the dominant E1 pec galaxy (de Vaucouleurs et al. 1991) in the center of the Fornax cluster. The ‘peculiarity’ of this galaxy is that it is a cD galaxy with an unusually extended stellar envelope. NGC 1399 is surrounded by a very rich population of globular clusters (Hanes & Harris 1986; Geisler & Forte 1990; Wagner et al. 1991; Bridges et al. 1991). The clusters have a bimodal color distribution, as confirmed independently by different groups (Ostrov, Geisler & Forte 1993; Kissler-Patig et al. 1997). Based on the photometry, these authors suggest two or more enrichment or formation episodes.

The only previous velocity measurements for globular clusters in NGC 1399 are those by Grillmair et al. (1994), who found a large velocity dispersion ($\sigma = 388 \pm 54 \text{ km s}^{-1}$). This velocity dispersion is larger than that of the Fornax cluster itself, which has $\sigma = 307 - 325 \text{ km s}^{-1}$ (Ferguson & Sandage 1990). The mean radial velocity of the clusters studied by Grillmair et al. is $v_{rad} = 1518 \pm 91 \text{ km s}^{-1}$, which is actually larger than that of NGC 1399 itself. They inferred a large M/L ratio for this galaxy, viz. $M/L = 79 \pm 20$.

Figure 1a displays the radial velocity distribution of the 47 globular clusters in NGC 1399 as measured by Grillmair et al. (1994). We notice that this velocity distribution is non-gaussian, and likely bimodal. The heliocentric radial velocity $v_{rad} = 1443 \text{ km s}^{-1}$ (Tully 1988) of the dominant galaxy NGC 1399 is close to the velocity of one of the peaks, while the other peak is close to the velocity of the nearby galaxy NGC 1404 with $v_{rad} = 1908 \text{ km s}^{-1}$, located at about 10 arcmin ($\sim 47 \text{ kpc}$) SE of the center of NGC 1399. For comparison, the velocities listed in the RC3 (de Vaucouleurs et al. 1991) for these galaxies are for NGC 1399: $v_{rad}(GSR) = 1323 \text{ km s}^{-1}$, $v_{rad}(opt) = 1447 \text{ km s}^{-1}$ and for NGC 1404: $v_{rad}(GSR) = 1805 \text{ km s}^{-1}$, $v_{rad}(opt) = 1929 \text{ km s}^{-1}$.

Figure 1b displays the radial velocity distribution of 67 galaxy members of the Fornax cluster, as measured by Ferguson (1989). We also noticed that the velocity distribution of these galaxies appears non-gaussian. The radial velocity of NGC 1399 seems to be offset from the mean velocity of the Fornax cluster, being smaller by about $100 - 200 \text{ km s}^{-1}$, depending on the adopted velocity of this galaxy: e.g., Ferguson (1989) takes $v_{rad} = 1430 \text{ km s}^{-1}$. This offset is not surprising, given that the centroid of the X-ray emission of the Fornax cluster is also offset from NGC 1399 (Ikebe et al. 1997). It is well known that some central galaxies are displaced from the center of their corresponding cluster potential well (cf. Hill et al. 1988; Beers et al. 1991; Oegerle & Hill 1994), and this is usually taken as an indication of substructure within the clusters (see the analysis by Bird 1994).

Given these indications of a complex system, the goal of this paper is two-fold:

1. to measure the radial velocities of a selected sample of globular clusters around NGC 1399 and to investigate the kinematics of the globular cluster system;
2. to derive, from the velocity dispersion of these globular clusters, the M/L for this galaxy at a radius intermediate between those probed by the galaxy integrated light and by the X-ray-emitting gas.

2. Selection of the Sample

Defining a sample of globular clusters that traces the galaxy rather than the galaxy cluster potential is important, since some globulars may have been stripped away from galaxies and populate the intergalactic medium (Muzzio 1987; Bassino et al. 1994; West et al. 1994). For example, Theuns & Warren (1997) showed evidence for intergalactic stars in the Fornax cluster, based on the discovery of 10 planetary nebulae. In relation to this, the X-ray emission mapped by ASCA has been interpreted as the superposition of concentrated emission from NGC 1399 itself, and more extended emission from the whole galaxy cluster (Ikebe et al. 1996).

There are observational indications that the kinematics of a globular cluster system may well depend on metallicity. For example, in the specific case of the merger NGC 5128, Hui et al. (1995) combined the NGC 5128 globular cluster velocities from Harris et al. (1988) and Sharples (1988) with the photometry of Harris et al. (1992). Dividing up the sample at $[\text{Fe}/\text{H}] = -1$ into a metal-poor and a metal-rich sample, they showed that the metal-rich globular cluster system of NGC 5128 rotates more rapidly and has smaller velocity dispersion than the metal-poor one. This is consistent with the fact that the metal-rich globular clusters are more centrally concentrated (Minniti et al. 1996).

Indeed, metal-rich clusters appear to be better tracers of the underlying metal-rich stellar populations, in elliptical galaxies (e.g., Forbes et al. 1997a) as well as in the Milky Way bulge (e.g., Minniti 1995). In order to study the kinematics of this population, we select metal-rich clusters in NGC 1399 on the basis of the colors measured by Kissler-Patig et al. (1997). The color distribution of NGC 1399 globular clusters is bimodal (Ostrov, Geisler & Forte 1993; Kissler-Patig et al. 1997). The color distribution shown by Kissler-Patig et al. (1997) ranges from about $V - I = 0.5$ to 1.5, with peaks at $V - I = 0.9$ and 1.2, the second peak corresponding to the mean color of the integrated light of NGC 1399 ($V - I = 1.24$, Poulain 1988). It is worth mentioning that the absolute location of these peaks in terms of $[\text{Fe}/\text{H}]$ is uncertain due to the age-metallicity degeneracy of optical colors (see, e.g., Worthey 1994, Vazdekis et al. 1996). However, the two strong peaks differ by more than $\Delta [\text{Fe}/\text{H}] = 0.5$ dex in the mean if interpreted as a pure metallicity difference.

We selected globular cluster candidates over the whole color range mentioned above (see Figure 2), focusing on metal-rich globular clusters which should have stronger spectral lines, which is an advantage for measuring radial velocities. These red candidates have $1.0 < (V - I)_0 < 1.5$, where we have adopted $E_{V-I} = 0.02$ for this field (Kohle et al. 1996). These colors are equivalent to selecting clusters with $[\text{Fe}/\text{H}] \gtrsim -1.0$ (see Kissler-Patig et al. 1997, their Figure 4), or a population similar to the metal-rich globular clusters associated with the Milky Way bulge (Minniti 1995).

We included a few candidates in the range $0.7 < (V-I)_0 < 1.0$, but all turned out to be stars, or to have too weak metal lines to measure good velocities. We further included even bluer and slightly brighter objects, in order to check whether NGC 1399 is hosting young- or intermediate-age globular clusters as seen in recent mergers (e.g., NGC 7252, [Whitmore et al. 1993], NGC 1275, [Holtzman et al. 1992; Nørgaard-Nielsen et al. 1993], NGC 5128, [Minniti et al. 1996] or NGC 5018 [Hilker & Kissler-Patig 1996]). All of our selected best candidates had good enough spectra to identify them as clear foreground stars and exclude the hypothesis of younger globular clusters.

Finally, we included very red objects with $(V-I)_0 > 1.5$, usually discarded in color distributions as background objects, in order to confirm their non-globular cluster nature. Here too the test was successful in the sense that very red objects indeed turned out to be either M stars or background galaxies, and neither very metal-rich, nor reddened globular clusters. Note that the errors in our photometry are small ($\sigma_{V-I} < 0.04$ mag at $18.5 < V < 21$), which is essential for the selection of clusters belonging to the metal-rich tail of the color distribution, and to the other groups considered.

As to the magnitude limit, we adopt for NGC 1399 a distance modulus of $m - M = 31.0$ after Kohle et al. (1996). At this distance, 1 arcmin corresponds to 4.6 kpc. This distance modulus is intermediate between the distance moduli of 30.6 and 31.5, adopted by Grillmair et al. (1994) and Ikebe et al. (1996), respectively. Therefore, in order to minimize foreground objects but to be complete at the bright end of the globular cluster luminosity function, we chose objects with $V > 18.5$ (corresponding to $M_V < -12.5$), except for the very blue objects that were assumed to be potential young globular clusters, and therefore brighter, for which we chose candidates with $16.5 < V < 18.5$ (i.e. $-12.5 < M_V < -14.5$). Figure 2 shows the color-magnitude diagram of 18 globular clusters with available spectra, along with 26 foreground stars. The color distribution of objects in the field of NGC 1399 from Kissler-Patig et al. (1997) is shown for comparison.

These tests indicate that globular cluster sample selection based on accurate magnitude and color limits can be very successful in deriving a clean globular cluster sample.

3. Observations

Spectroscopy of NGC 1399 clusters was carried out during four half-nights, in late 1995 and early 1996, with the ESO 3.5-m New Technology Telescope (NTT) equipped with the ESO Multi-Mode Instrument (EMMI) in Multi-Object Spectroscopy (MOS) mode.

The detector was a thin, back-illuminated CCD of type Tektronix TK2048EB Grade

2, having 2048×2048 pixels (of size $24 \mu\text{m} = 0''.268 \text{ pixel}^{-1}$). We used grism No. 4 ($2.8 \text{ \AA pixel}^{-1}$, blazed at 6500 \AA). The wavelength range is $5500 - 10000 \text{ \AA}$, although the actual wavelength coverage of the individual spectra varied according to the location of the slitlets in the MOS masks. The slitlets had a width of $1''.34$, resulting in a spectral resolution of 7.5 \AA .

We decided to take spectra in the spectral range including the Ca II triplet ($\lambda\lambda 8498, 8542, 8662 \text{ \AA}$) since the Ca II index is an excellent metallicity indicator, being independent of age for objects older than about 1 Gyr (Bica & Alloin 1987, Armandroff & Zinn 1988). Unfortunately, the majority of our spectra do not have high enough S/N ratios to allow accurate metallicity abundance measurements.

Astrometry and photometry for the observed globular cluster candidates in NGC 1399 is available from Kissler-Patig et al. (1997). However, precise astrometry for MOS targets alone is not sufficient to produce MOS plates, since an accurate map of the distortion in the focal plane of the NTT was not available. To overcome this problem, short-exposure (R band, exp. time = 5 min) “acquisition” images were kindly taken in advance by J. van Loon, from which the (x, y) positions of our targets were derived to produce the MOS masks.

The effective punching area for the MOS masks is $5' \times 8'$. Three MOS masks were made to include the maximum possible number of globular cluster candidates during the available time. In each mask, two or three slitlets were punched at positions corresponding to bright “reference” Galactic stars in the field of view, which were used to check the precision of the telescope pointing.

Spectra were taken on October 7, 1995 for a field centered NE of NGC 1399 (our field 2), with a total exposure time of 150 minutes. The seeing was $1''.0$, as judged from the direct image immediately preceding the MOS observation. Spectra for a field centered NW of NGC 1399 (our field 4) were obtained on November 7, 1995, with a seeing of $0''.9$ and a total exposure time of 135 minutes, and the spectra for a field centered SE of NGC 1399 (our field 1) were obtained on January 30 and January 31, 1996, with an average seeing of $0''.9$ and a total exposure time of $130 + 110$ minutes in the two half-nights.

Multiple exposures were acquired during each night. Individual exposures were typically of 1800-s duration, and interleaved with short imaging exposures to correct for small pointing errors due to e.g., flexure and differential atmospheric refraction (the corrections needed were only of order $0''.3$ or smaller; the airmass was always below 1.3).

The third mask, located in the SE of NGC 1399, has twice as many coadded exposures (6) than the other two masks, located at the NW and NE of the center of this galaxy.

Therefore, we were able to extract more spectra in the SE field, and with higher S/N ratios. On the other hand, the NW field had the lowest S/N and objects fainter than $V = 20.7$ could barely be measured. The SW field could not be observed due to lack of time.

The observations were made during bright time, with typical sky surface brightness of $\mu_I = 19.2$ mag/arcsec². The underlying “background” brightness of the galaxy is more problematic only in the inner regions of NGC 1399, where some of the targets are located: E.g., $\mu_I = 18.5$ mag/arcsec² at 25 arcsec from the galaxy center (Goudfrooij et al. 1994). These objects require a longer exposure time, and the large background variations account for a wide range of S/N ratios achieved in the different spectra.

4. Data Reduction

A total of 20 bias frames were taken in the afternoon of each observing night. These were averaged together to form a “superbias” frame, in which the effect of read-out noise is rendered negligible. The superbias frame was subtracted from each “science” frame, after having been properly scaled to match the bias level in the serial overscan region of each observation. Multiple dome flat field exposures were obtained for each MOS mask with the grism in place, using an external lamp. After combining the flat field images for each individual mask, the flat fields were normalized to an average value of unity. This was done for each slitlet individually by dividing the measured wavelength response of the flat field lamp by a third-order polynomial fit.

The two-dimensional spectra of each star and cluster candidate were extracted from the flatfielded MOS frames and wavelength calibrated using the corresponding He-Ar calibration lamp exposure. Residual zeropoint errors were corrected using the night-sky lines which are numerous and prominent in the wavelength region covered. The extracted spectra were combined and appeared largely free of cosmic ray hits; the few residual affected pixels were interpolated over by hand. The sky background was derived for each target individually by fitting a Chebyshev polynomial to the background regions in the slitlets, along as well as perpendicular to the dispersion. The fitted background spectrum was then subtracted from each individual spectrum.

The final spectra were cross-correlated with 2-3 stellar template spectra using the method of Tonry & Davis (1979), incorporated in the package FXCOR within IRAF. Night-sky lines, which are very numerous and prominent in the wavelength region covered, were used for the zero-point of the individual templates observed simultaneously with the same setup. Although no radial velocity standards from the IAU lists were observed, the

zero point of our velocities is good to 50 km s^{-1} . Cross-correlation peaks with $R < 2.5$ (this is the R ratio of Tonry and Davis 1979, defined as the relative height of the main cross-correlation peak with respect to the neighboring peaks), were discarded, as their velocities are not reliable enough, judging from the cross correlations against the different templates. A total of 6 objects did not yield spectra with a S/N ratio high enough to meet this criterion. The typical FWHM of the cross-correlation peaks is about 500 km s^{-1} , and the abscissa of the peak itself is defined to better than 100 km s^{-1} . Although the Ca II triplet used to measure radial velocities is usually very strong in globular cluster spectra, it is weaker in the metal-poor globulars. Therefore, we have concentrated on the metal-rich ones, for which velocities can be measured with higher confidence in relatively shorter exposure times.

Table 1 lists the globular cluster data: column 1 contains the object ID, columns 2, 3, 4 and 5 contain the x and y coordinates in arcsec from the center of the galaxy, and the J1950 equatorial coordinates, respectively, following Kissler-Patig et al. (1997); columns 6 and 7 list their magnitudes and colors, respectively; column 8 lists the heliocentric radial velocities in km s^{-1} ; columns 10 and 11 list the errors Δ_{Vr} and ϵ_{Vr} , corresponding to the maximum difference in velocities computed with respect to the various templates, and these given by the cross correlations package, respectively. Table 2 lists similar data for the background galaxies and foreground stars in our sample. Their classifications are listed in the last column.

We cross-checked the positions of our globular clusters with those of Grillmair et al. (1994), finding two objects in common, #119 and #406. The velocity differences for these clusters are $\Delta V = 57$ and -63 km s^{-1} , respectively, showing good consistency. A couple of fainter cluster candidates that are included in the list of Grillmair et al. (1994) had too low S/N to provide accurate velocities.

5. Foreground Stars in the Sample

We obtained spectra for 28 stars (see Table 2), some of which (7) were deliberately chosen as standard stars (to use as pointing check and as radial velocity templates), and some (21) turned out to be failed young cluster candidates and reddened or super metal-rich cluster candidates. These spectra turn out to be very useful also to estimate the uncertainties, as discussed below.

Figure 3 shows the dependence of the radial velocity on the V magnitudes and $V-I$ colors for the foreground stars and the NGC 1399 clusters. There is a clear segregation

in radial velocity between the foreground stars and the globular clusters and background galaxies. All objects with $v_{rad} \lesssim 400$ km s $^{-1}$ are foreground stars and all objects brighter than $V \sim 19.5$ are foreground stars or galaxies, but *not* globular clusters.

The mean velocity of the foreground stars ($v_{rad} = 65 \pm 27$ km s $^{-1}$, $N = 28$) matches the expected velocity of halo stars in this direction of the sky ($v_{rad} = 220 \cos l \sin b = 110$ km s $^{-1}$). Sommer-Larsen (1987) predicts, in this direction of the sky, a mean velocity and velocity dispersion of $v_{rad} = 110$ km s $^{-1}$ and $\sigma = 115$ km s $^{-1}$, respectively. These values are confirmed – to within the errors – by a small sample of stars ($N = 6$) measured in this field by Grillmair et al. (1994), who give $v_{rad} = 144 \pm 254$ km s $^{-1}$ and $\sigma = 269 \pm 167$ km s $^{-1}$.

The intrinsic velocity error can also be estimated by comparing the observed stellar velocity dispersion ($\sigma = 143 \pm 19$, $N = 28$) with that expected for the MW stars along this line-of-sight ($\sigma = 115$, cf. Sommer-Larsen 1987). Subtracting these in quadrature we obtain an intrinsic error per measurement of $\sigma_0 = 85$ km s $^{-1}$, which agrees with the typical errors listed in Table 1. This should be considered an optimistic estimate of the errors, because the stars are brighter than the globular clusters in the mean.

We can also divide up the stellar sample according to their brightness (see Figure 3). The 11 stars with $V < 18$ have $v_{rad} = 53 \pm 17$ km s $^{-1}$, and $\sigma = 56 \pm 12$ km s $^{-1}$, consistent with a mixture of foreground disk and halo dwarf stars. The fainter stars with $18 < V < 21$ have $v_{rad} = 72 \pm 44$ km s $^{-1}$, and $\sigma = 180 \pm 31$ km s $^{-1}$, consistent with a dominant halo population. This difference in velocity dispersion between the two subsamples persists even if we take into account that the fainter stars have larger errors. However, there are no detailed kinematic studies published for such faint stars to compare with these results.

6. Globular Cluster Results

For the adopted distance modulus of NGC 1399, viz. $m - M = 31.0$ (Kohle et al. 1996), the brightest globular clusters members of NGC 1399 have, in our sample, $V \sim 19.5$ i.e. $M_V = -11.5$. This is significantly brighter than the brightest globular clusters in the Galaxy and M31, viz. ω Centauri with $M_V = -10.07$, and Mayall II = G1 with $M_V = -10.55$, respectively. However, more luminous globular clusters with $M_V \leq -10.7$ are known in other well studied giant galaxies from photometric (e.g., Whitmore et al. 1995; Elson et al. 1996), and spectroscopic studies (e.g. Mould et al. 1990). Note that the object at $V = 18.5$, $V - I = 1.48$ (our reddest “globular cluster”), which has $M_V = -12.5$ was identified as a compact dwarf galaxy on the images after light profile analysis (Hilker priv. com.). We will include this object in the subsequent analysis.

A relaxed virialized system will have a near-Maxwellian velocity distribution, which implies that the observed radial velocity distribution should be Gaussian to a first approximation. Figure 4 shows the velocity distribution for our sample of 18 globular clusters in the field of NGC 1399. This velocity distribution is different in appearance from that of Grillmair et al. (1994, Fig. 1). Given the small number of objects, however, the difference is not statistically significant. Figure 4 shows one dominant peak at $v_{rad} \sim 1350$ km s $^{-1}$, which is coincident with the lowest peak of their distribution. Fitting a Gaussian to this distribution gives $v_{rad} = 1353 \pm 79$ km s $^{-1}$, and $\sigma = 338 \pm 56$ km s $^{-1}$ for $N = 18$ objects. We argue that this value for σ may have no great physical meaning because (i) the velocity distribution may not be Gaussian (as it shows two peaks, Grillmair et al. 1994), and (ii) there could be some contamination by globular clusters associated either with NGC 1404 or with the intergalactic medium.

The globular cluster system of NGC 1404 was studied by Richtler et al. (1992), Hanes & Harris (1986), Forbes et al. (1997b), and Blakeslee & Tonry (1996). In particular, Forbes et al. (1997b) suggest that a large fraction of intermediate-metallicity clusters may have been stripped by NGC 1399, in order to account for the low specific frequency of globulars in NGC 1404. In fact, some of the clusters populating the high velocity tail of the distribution are indeed located in the direction of NGC 1404. Note that with a larger sample we should be able to distinguish whether the possible bimodality is indeed due to contamination from NGC 1404, or if this is due to all the clusters being in nearly circular orbits. The latter situation has been argued to be appropriate for the galaxy M49 (NGC 4472), which also has a bimodal velocity distribution with peaks separated by about 500 km s $^{-1}$ (Mould et al. 1990).

If we eliminate the cluster with highest radial velocity, arguing that it is a potential member of NGC 1404 or the Fornax cluster of galaxies itself, then $v_{rad} = 1309 \pm 71$ km s $^{-1}$, and $\sigma = 293 \pm 50$ km s $^{-1}$ for $N = 17$ objects. Figure 5 shows the radial dependence of velocity dispersion for different tracers in the field of NGC 1399. These tracers include the integrated stellar light (from Franx et al. 1989; Bicknell et al. 1989; Winsall & Freeman 1993), planetary nebulae (from Arnaboldi et al. 1994), globular clusters (from Grillmair et al. 1994, and the present paper), and galaxies belonging to the Fornax cluster (from Ferguson 1989). Our values of σ , computed using $N=17$ and $N=18$ objects, follow the trend of the integrated light from the galaxy.

Arnaboldi et al. (1994) have detected a rotation in the system of planetary nebulae in the NGC 1399 halo. They measure a rotation curve with 1.09 km s $^{-1}$ arcsec $^{-1}$ and position angle -35° . Accepting this figure rotation does not change the velocity dispersion of the present cluster system significantly, although the mean velocity in field 1 is lower than that

of field 4, showing the opposite effect. The present sample lacks objects in the SW region, and is more extended in the NW-SE direction, as shown in Figure 6. More radial velocity measurements with adequate spatial distribution are needed to derive a figure rotation for the metal-rich cluster system of NGC 1399. In addition, any fitting for rotation would have to assess the probability of contamination from the clusters associated with the nearby elliptical NGC 1404 and/or the intergalactic medium.

We can use one of the Jeans equations of stellar dynamics (Binney & Tremaine 1987), in order to estimate the mass of the system:

$$M(r) = -\frac{\sigma_r^2 r}{G} (d \ln \rho / d \ln r + d \ln \sigma_r^2 / d \ln r + 2\beta),$$

where $M(r)$ is the total mass inside the radius r , σ_r is the radial component of the velocity dispersion of the test particles, ρ is the spatial density of the test particles, and $\beta = 1 - \sigma_\theta^2 / \sigma_r^2$ is a measure of the degree of anisotropy of the velocity distribution at each point. Given the lack of observational constraints on the radial gradient of the velocity dispersion, we consider the simplifying hypotheses of isothermality and isotropy, i.e. $\sigma_r = \sigma$, $d \ln \rho / d \ln r = 0$, and $\beta = 0$.

Another question concerns the spatial distribution of the clusters. The spatial distribution of the NGC 1399 cluster system has been studied by Ostrov, Geisler, & Forte (1993) and Kissler-Patig et al. (1997). The total surface density profile follows a power law of with $n = -1.7$. The globular clusters in NGC 1399 follow a clearly flatter distribution than in nearby smaller ellipticals; however, the distribution still matches that of the galaxy light due to the extended cD envelope of NGC 1399 (Kissler-Patig et al. 1997). No clear difference between the spatial distribution of the blue and red globular cluster populations have been found.

Grillmair et al. (1994) used the Jeans equation, adopting spherical symmetry and circular orbits, in order to compute a lower limit of $M/L = 79 \pm 20$ for the cluster system of NGC 1399. The velocity dispersion found here implies a slightly smaller M/L : since $M \propto \sigma^2$, the M/L value corresponding to $\sigma = 388 \text{ km s}^{-1}$ of Grillmair et al. (1994) yields $M/L \sim 60$ for $\sigma = 338 \text{ km s}^{-1}$. However, since $M/L \propto \text{distance}$, and since we have adopted a distance modulus $m - M_0 = 31.0$ which is 0.4 mag larger than that of Grillmair et al. (1994), this value would be reduced further to $M/L = 50$.

We have used the projected mass estimator (Heisler et al. 1985), again under the hypothesis of a spherical distribution of matter and isotropy of the velocity dispersion (see Perelmutter et al. 1995 and Bridges et al. 1997 for similar applications of this method to

other galaxies). The projected mass M_P for an isotropic velocity ellipsoid is:

$$M_P = \frac{32}{\pi NG} \times \Sigma_1^{18} (v_i - v_o)^2 R_i,$$

where v_i is the radial velocity of the considered globular cluster, v_o is either the radial velocity of the galaxy or the mean radial velocity of the cluster sample, and R_i the globular cluster distance on the plane of the sky from the center of the galaxy. For the 18 globular clusters with a mean radial velocity of 1353 km s^{-1} for which $\sigma = 338 \pm 56$, we obtain $M_P = 5.0 \times 10^{12} M_\odot$. This mass estimate, along with $L = 3.9 \times 10^{10} L_\odot$ (Grillmair et al. 1994, scaled to our adopted distance), gives $M_P/L \sim 129$. The error in this quantity is dominated by the small sample size and the different underlying theoretical assumptions. E.g., adopting radial instead of isotropic orbits for the globular clusters increases the mass estimate by a factor of two.

Other mass estimators (Heisler et al. 1985) applied to the same sample give the following results: the virial mass $M_{VT} = 4.2 \times 10^{12} M_\odot$ implies $M_{VT}/L \sim 109$, the median mass $M_M = 3.3 \times 10^{12} M_\odot$ implies $M_M/L \sim 87$, and the average mass $M_{AV} = 4.2 \times 10^{12} M_\odot$ implies $M/L \sim 109$. The virial, projected, and average masses share the same sensitivity to interlopers. For example, if there are interlopers from the intracluster medium, or from the nearby galaxy NGC 1404, these would tend to have higher velocities. Eliminating the object with the largest radial velocity (#407 with $V_r = 2107 \text{ km s}^{-1}$) from the present sample of 18 globular clusters, the above M/L values decrease to $M_P/L \sim 81$ for projected mass, $M_{VT/L} \sim 78$ for virial mass, $M_M/L \sim 68$ for median mass, and $M_{AV/L} \sim 67$ average mass. These M/L values, obtained from the globular cluster system of NGC 1399, are similar to the corresponding values obtained with the same mass estimators by Huchra & Brodie (1987) from the globular cluster system of M87.

Contrary to the velocity dispersion determinations, which suffer only from the observational errors on the radial velocities, the mass-to-luminosity estimates accumulate the errors associated with many various observed parameters, such as the total luminosity within a given radius, the distance modulus and the radial velocity of the host galaxy, not to mention the different theoretical assumptions. Considering the large uncertainties on the M/L determinations, reliable comparisons with the earlier study by Grillmair et al. (1994) can be made only for the above determination using similar assumptions, namely use of the Jeans equation and providing $M/L \sim 50$. This value is somewhat smaller than those reported in previous studies at large distance from the center of NGC 1399, but it is in accord with the M/L values computed from the X-ray emission (Ikebe et al. 1996). Note that this value of M/L is larger than that of a typical old stellar population ($1 < M/L < 10$), supporting the existence of dark matter. We also confirm that M/L increases with radius, ruling out a constant M/L . A similar result, although much more

accurate due to the large number of high quality *Keck* spectra available, is obtained by Cohen & Ryzhov (1997) for the cluster system of M87. The same conclusion can be reached by looking at Figure 5, which shows that our velocity dispersion measurement is intermediate between those from the outermost integrated stellar light (from Franx et al. 1989; Bicknell et al. 1989; Winsall & Freeman 1993) and the estimate from velocities of galaxies belonging to the Fornax cluster (from Ferguson 1989).

7. Conclusions

We have measured velocities for 53 objects in the field of NGC 1399, including 7 background galaxies, one dwarf galaxy in Fornax, 18 globular cluster candidates, and 28 foreground stars. Located in the central region of the Fornax cluster of galaxies, NGC 1399 is a particularly interesting system to use as a reference, because it does not seem to host young or intermediate age globular clusters as seen in recent or past mergers such as NGC 7252, NGC 1275, NGC 5128 or NGC 5018. The main conclusions are:

- We find that all candidates with $V < 19.5$ are either foreground stars or background galaxies, and *not* young globular clusters. We also find that the very red ($(V-I)_0 > 1.5$) objects in the color distribution are *not* (very metal-rich or reddened) globular clusters.
- The radial velocity distribution of metal rich globular clusters is different from the distribution of the whole population. In particular, it shows a dominant peak centered on the radial velocity of NGC 1399 itself.
- Assuming that the metal-rich globular clusters are a better tracer of the underlying galaxy than the metal-poor ones, we have a sample that better traces the potential of this galaxy. We derive a velocity dispersion of $\sigma = 338 \pm 56 \text{ km s}^{-1}$ (or $\sigma = 293 \pm 50 \text{ km s}^{-1}$ eliminating the cluster with largest velocity). These values are somewhat smaller than that measured by Grillmair et al. (1994), who did not discriminate against more metal-poor globular clusters.
- The kinematics of the globular cluster system of NGC 1399 are complicated, which is perhaps related to the presence of different populations as inferred from the bimodal color distribution, and assumptions of dynamical equilibrium or isotropy of the whole system are not warranted. In particular, we note that NGC 1399 is offset from the center of the Fornax cluster potential well, both in velocity and in position in the sky. This suggests the presence of substructure in the Fornax cluster, and in order to unravel the dynamics of the system, velocities for more tracers are needed.

- Ignoring the previous conclusion, we derive, in a way similar to Grillmair et al. (1994), an estimate of $M/L \sim 50$ at a mean distance of $r = 5.5$ arcmin. This value joins nicely the measurements based on the integrated galaxy light in the inner regions with those based on recent X-ray emission measurements in the outer regions (Ikebe et al. 1996). This would argue for M/L increasing with radius in this galaxy, though at more moderate rates than previously thought. Other mass estimators provide M/L in the range 50-130, although with large uncertainties.

The total number of data points is too small to do a comprehensive statistical analysis, as $N > 50$ points are required (e.g. Bird 1994). Consequently, larger radial velocity samples are needed. Until they become available, we can neither precisely evaluate the rotation of the metal-rich globular cluster population, nor investigate its dynamics. Other questions that remain to be answered are (i) the extent to which clusters that belong to NGC 1404 contribute to the measured dispersions, and (ii) whether or not some clusters from NGC 1404 been stripped by NGC 1399 in the past, as proposed by Forbes et al. (1997b). We speculate that the more metal-poor clusters may be responsible for the larger velocity dispersion, and therefore should have a more extended spatial distribution than the more metal-rich ones. This would support the possibility that some of these metal-poor clusters belong to the intragalactic medium of the Fornax cluster, as suggested by Muzzio (1987), Grillmair et al. (1994), and West et al. (1995).

We would like to thank J. Rodriguez, V. Reyes, and the whole NTT team for their expert and efficient support. We thank Jacco van Loon for taking acquisition exposures for us, and D. Geisler for useful comments. Work performed at IGPP-LLNL is supported by the DOE under contract W7405-ENG-48. MKP acknowledges the supported by the DFG through the Graduiertenkolleg ‘The Magellanic System and other dwarf galaxies’, as well as the hospitality of IGPP-LLNL during which part of this work was done.

REFERENCES

Armandroff, T., & Zinn, R. 1988, AJ, 96, 92
Arnaboldi, M., Freeman, K. C., Hui, X., Capaccioli, M., & Ford, H. 1994, ESO Messenger, 76, 40
Ashman, K. M., & Bird, C. M. 1993, AJ, 106, 2281
Ashman, K. M., Zepf, S. E. 1992, ApJ, 384, 50
Baum, W.A., 1955 PASP, 67, 328

Bassino, L. P., Muzzio, J. C., & Rabolli, M. 1994 *ApJ*, 431, 634

Beers, T. C., et al. 1991, *AJ*, 102, 1581

Bica, E., & Alloin, D. 1987, *A&A*, 186, 49

Bicknell, G. V., Carter, D., Killeen, N., & Bruce, T. 1989, *ApJ*, 336, 639

Binney, J., & Tremaine, S. 1997, *Galactic Dynamics* (Princeton University Press)

Bird, C. 1994, *AJ*, 107, 1637

Blakeslee, J. P., & Tonry, J. 1996, *ApJ*, 465, L19

Bridges, T. J., Ashman, K., Zepf, S., et al. 1997, *MNRAS*, in press

Bridges, T. J., Hanes, D. A., & Harris, W. E. 1991, *AJ*, 101, 469

Cohen, J. G., & Ryzhov, A. 1997, *AJ*, in press (astro-ph/9704051)

de Vaucouleurs, G. H., de Vaucouleurs, A., Corwin, H. G., Buta, R. J., Paturel, G., Fouqué, P. 1991, “Third Reference Catalog of Bright Galaxies” (New York: Springer)

Durrell, P., Harris, W., Geisler, D. et al. 1996, *AJ*, 112, 972

Elson, R. A. W., & Santiago, B. X. 1996, *MNRAS*, 278, 617

Ferguson, H. C. 1989, *AJ*, 98, 367

Ferguson, H. C., & Sandage, A. 1990, *AJ*, 100, 1

Forbes, D. A., Brodie, J. P., & Grillmair, C. J. 1997a, *AJ*, in press

Forbes, D. A., Brodie, J. P., & Huchra, J. 1997b, *AJ*, in press

Forte, J. C., Strom, S. E., & Strom, K. M. 1981, *ApJ*, 418, L55

Franx, M., Illingworth, G., & Heckman, T. 1989, *ApJ*, 344, 613

Geisler, D., Lee, M. G., & Kim, E. 1996, *AJ*, 111, 1529

Geisler, D., & Forte, J. C. 1990, *ApJ*, 350, L5

Goudfrooij, P. et al. 1994, *A&AS*, 104, 179

Grillmair, C. J., Freeman, K., C., et al. 1994, *ApJ*, 422, L9

Hanes, D. A., & Harris, W. E. 1986, *ApJ*, 309, 564

Hanes, D. A., & Harris, W. E. 1986, *ApJ*, 309, 599

Harris, W. E. 1991, *ARA&A*, 29, 543

Harris, W. E. 1995, in *IAU Symp.* 164, p. 85

Harris, W. E., & Hanes, D. A. 1987, *AJ*, 93, 1368

Harris, W. E., Harris, G. L. H., & Hesser, J. E. 1988, IAU Symp. 126, p. 215

Heisler, J., Tremaine, S., & Bahcall, J. N. 1985, ApJ, 298, 8

Hill, J. M., Hintzen, P., Oegerle, W. R., Romanishin, W., Lesser, M. P., Eisenhamer, J. D., & Batuski, D. J. 1988, ApJ, 332, L23

Holtzman, J. A., et al. 1992, AJ, 103, 691

Huchra, J., & Brodie, J. 1987, AJ, 93, 779

Hui, X., Ford, H. C., Freeman, K. C., & Dopita, M. A. 1995, ApJ, 449, 592

Ikebe, Y., et al. 1996, Nature, 379, 427

Kissler-Patig, M. 1997, A&A, 319, 83

Kissler-Patig, M., Kohle, S., M. Hilker, Richtler, T., et al. 1997, A&A, 319, 470

Kohle, S., Kissler-Patig, M., Hilker, M., Richtler, T. R., Infante, L., Quintana, H. 1996, A&A, 309, L39

Minniti, D. 1995, AJ, 109, 1663

Minniti, D., Alonso, M. V., Goudfrooij, P., Meylan, G., & Jablonka, P. 1996, ApJ, 467, 221

Mould, J., Oke, J. B., & Nemec, J. M. 1987, AJ, 92, 53

Mould, J., Oke, J. B., de Zeeuw, P. T., & Nemec, J. M. 1990, AJ, 99, 1823

Muzzio, J. C. 1987, PASP, 99, 245

Nørgaard-Nielsen, H. U., Goudfrooij, P., Jørgensen, H. E., & Hansen, L. 1993, A&A, 279, 61

Oegerle, W. R., & Hill, J. M. 1994, AJ, 107, 857

Ostrov, P., Geisler, D., & Forte, J. C. 1994, AJ, 105, 1762

Poulain, P., 1988, A&AS, 772, 215

Racine, R., 1968, PASP 80, 326

Richtler, T., Grebel, E. K., Domgorgen, H., Hilker, M., & Kissler, M. 1992, A&A, 264, 25

Sharples, R. 1988, IAU Symp. 126, p. 245

Sommer-Larsen, J. 1987, MNRAS, 227, 21P

Strom, S. E., Forte, J. C., Harris, W. E., Strom, K. M., Wells, D. C., & Smith, M. G. 1981, ApJ, 245, 416

Theuns, T., & Warren, S. J. 1997, MNRAS, 284, L11

Tonry, J., & Davis, M. 1979, AJ, 84, 1511

Tully, R. B. 1988, *Nearby Galaxies Catalog*, Cambridge University Press

van den Bergh, S. 1996, *PASP*, 108, 986

de Vaucouleurs, G., et al. 1991, *Revised Catalogue of Galaxies Version 3.9 (RC3.9)*

Vazdekis, A., Casuso, E., Peletier, R. F., Beckman, J. E. 1996, *ApJS*, 106, 307

Wagner, S., Richtler, T., & Hopp, U. 1991, *A&A*, 241, 399

West, M., et al. 1996, *ApJ*, 453, L77

Whitmore, B. C., Schweizer, F., Leitherer, C., Borne, K., & Robert, C. 1993, *AJ*, 106, 1354

Whitmore, B. C., & Schweizer, F. 1995, *AJ*, 109, 960

Whitmore, B. C., Sparks, W. B., Lucas, R. A., Macchetto, F. D., & Biretta, J. A. 1995, *ApJ*, 454, L73

Winsall, M., & Freeman, K. C. 1993, *A&A*, 268, 443

Worthey, G. 1994, *ApJS*, 95, 107

Zepf, S., & Ashman, K. 1993, *MNRAS*, 264, 611

Table 1. Globular Cluster Candidates

ID	X	Y	RA(1950)	DEC(1950)	V	V−I	v_{rad} [km/s]	Δ_{Vr}	ϵ_{Vr}	Class
201	529	−284	3 36 44.2	-35 35 40	21.17	1.24	1061	20	135	glob
203	1532	−548	3 37 02.9	-35 34 40	20.69	1.08	994	115	73	glob
208	1107	−1382	3 36 55.0	-35 31 31	20.91	1.12	1275	44	91	glob
406	−669	−199	3 36 21.9	-35 35 60	20.55	1.11	917	19	55	glob
407	−1323	−450	3 36 09.8	-35 35 02	20.19	1.01	2107	—	159	glob
410	−897	−791	3 36 17.7	-35 33 45	19.83	1.27	1190	13	94	glob
414	−1013	−1077	3 36 15.5	-35 32 40	19.56	1.09	1565	—	105	glob
101	1129	1942	3 36 55.4	-35 44 05	—	—	1270	75	118	glob
103	745	1803	3 36 48.3	-35 43 34	19.59	0.63	2738	49	398	blue glob?
104	1308	1744	3 36 58.7	-35 43 21	18.51	1.48	1459	17	52	(glob) dE
109	1315	1325	3 36 58.9	-35 41 46	21.24	1.27	1249	29	103	glob
113	337	1061	3 36 40.7	-35 40 46	21.15	1.26	1440	22	138	glob
119	1468	410	3 37 01.7	-35 38 18	21.16	1.19	1349	20	105	glob
122	1564	257	3 37 03.5	-35 37 43	20.77	1.06	1731	52	92	glob
123	1060	206	3 36 54.1	-35 37 32	20.93	1.00	1307	29	164	glob
124	461	126	3 36 43.0	-35 37 14	21.18	1.25	1142	16	189	glob
125	355	68	3 36 41.0	-35 37 00	21.02	1.17	1772	16	142	glob
126	553	29	3 36 44.7	-35 36 52	20.76	1.22	723	132	207	glob
127	490	−57	3 36 43.5	-35 36 32	21.06	1.16	1811	33	95	glob

Table 2. Background Galaxies and Foreground Stars

ID	X	Y	V	V-I	v_{rad} [km/s]	Δ_{Vr}	ϵ_{Vr}	Class
116	993	1545	21.18	1.10	5400	—	—	faint gal?
117	877	1504	20.92	1.22	4560	—	—	faint gal?
118	1091	1390	21.17	1.28	3011	—	—	faint gal?
120	1131	330	21.65	1.72	2988	—	—	faint gal
404	−751	−73	21.77	1.89	3105	—	—	faint gal
412	−478	−898	20.70	1.10	4536:	—	—	gal?
418	−1084	−1678	20.59	0.83	2849	—	—	gal?
202	945	−452	17.94	0.83	4	39	24	star
204	1327	−716	14.45	0.58	50	30	14	ref star
205	1422	−816	19.14	1.78	142	69	51	star
207	828	−1105	<14	0.93	15	30	14	ref star
209	752	−1649	18.22	0.66	219	14	34	star
210	814	−1736	18.31	0.52	−35	42	44	star
211	932	−1809	20.40	1.89	−191	—	106	star
212	665	−1831	19.58	1.31	201	19	51	star
213	494	−1983	17.70	0.65	120	17	36	star
408	−1328	−491	20.29	1.69	32	5	70	star
409	−1438	−647	18.81	1.33	390	2	43	star
411	−1074	−815	19.81	1.59	133	3	56	star
413	−1209	−926	13.82	0.80	105	12	8	ref star
419	−964	−1702	18.82	1.34	88	15	48	star
420	−1227	−1790	13.33	0.36	88	12	8	ref star
415	−1549	−1113	19.50	0.91	144	13	15	star
416	−1086	−1540	16.76	0.97	107	21	20	star
417	−845	−1613	17.57	0.92	120	42	49	star
102	—	—	<14	—	−1	25	22	ref star
106	993	1545	19.24	1.33	72	22	92	star
107	877	1504	20.33	0.82	76	4	88	star
108	1091	1390	14.81	1.33	−24	25	22	ref star
110	1093	1270	19.80	1.74	91	22	95	star
111	640	1208	20.15	0.92	−349	43	284	star
112	1162	1160	18.99	2.38	11	27	100	star
114	863	796	20.73	1.73	−126	50	89	star
115	821	746	19.91	0.78	325	39	89	star
121	545	292	<14	—	1	25	22	ref star

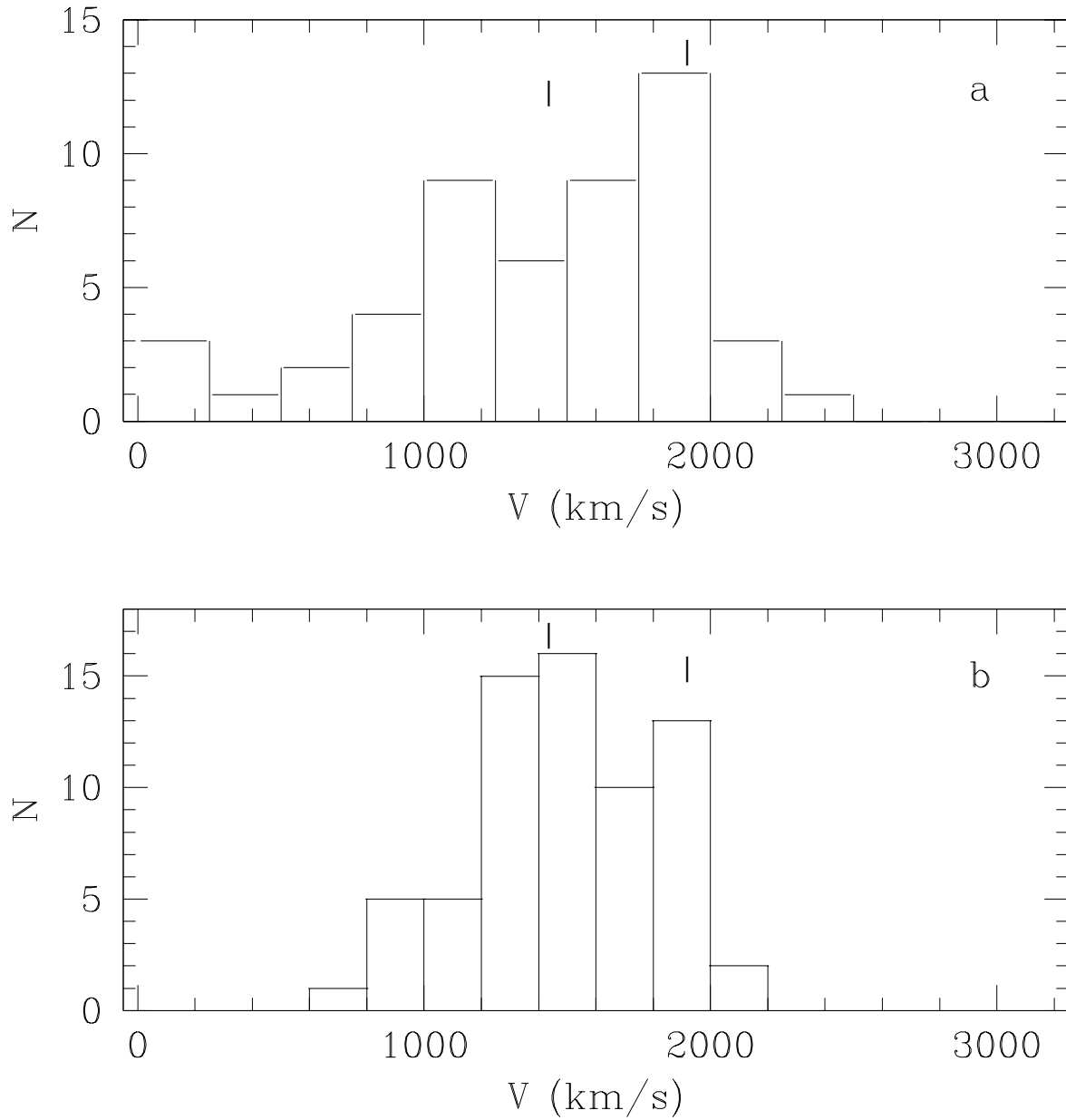


Fig. 1.— a) Radial velocity distribution for the globular clusters in NGC 1399, from Grillmair et al. (1994). b) Radial velocity distribution for the galaxies members of the Fornax cluster, from Ferguson (1989). The vertical tick marks in the figures, at $V = 1294$ and $V = 1944$, indicate the radial velocities of the galaxies NGC 1399 and NGC 1404, respectively.

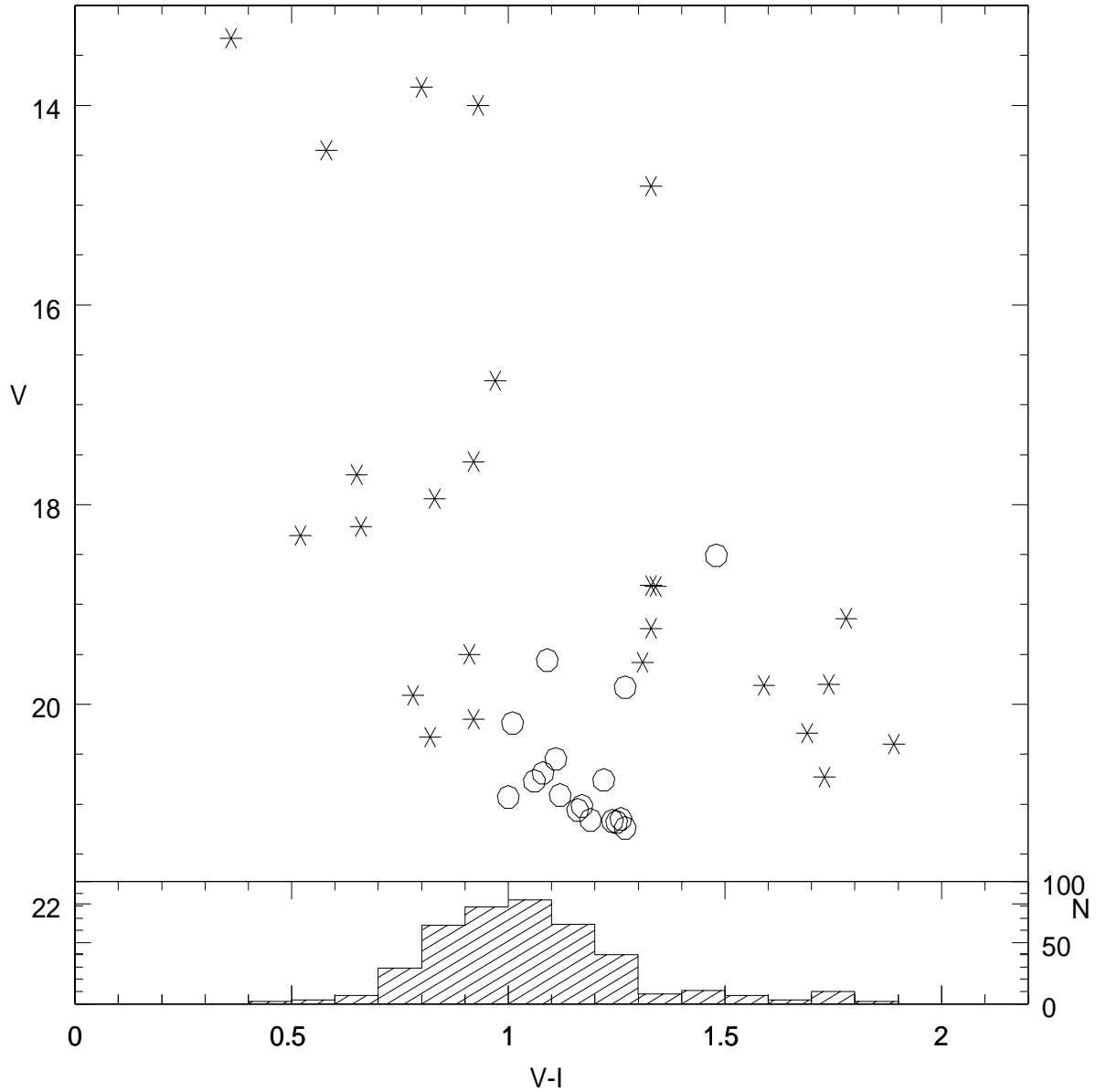


Fig. 2.— Optical color-magnitude diagram for the non-saturated stars (asterisks) and clusters (circles) of the sample. The brightest cluster candidate at $V = 18.5$, $V - I = 1.5$ may actually be a dE galaxy (see text). The color distribution of objects in the field of NGC 1399 is shown for comparison (from Kissler-Patig et al. 1997).

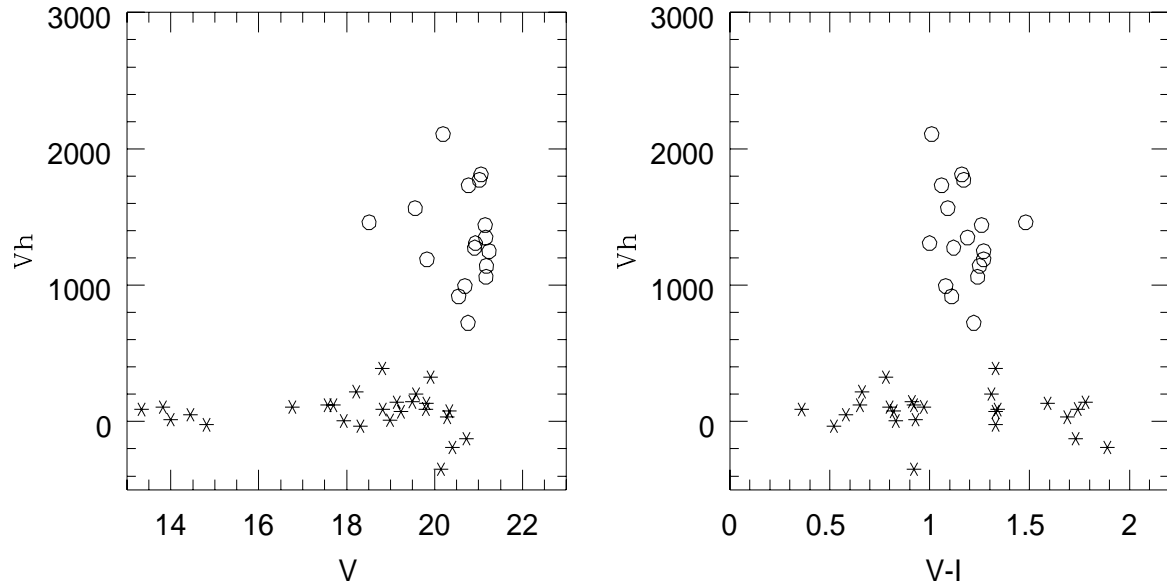


Fig. 3.— Dependence of velocity on V magnitude (left panel) and $V - I$ color (right panel) for the stars (asterisks) and clusters (circles) of the sample.

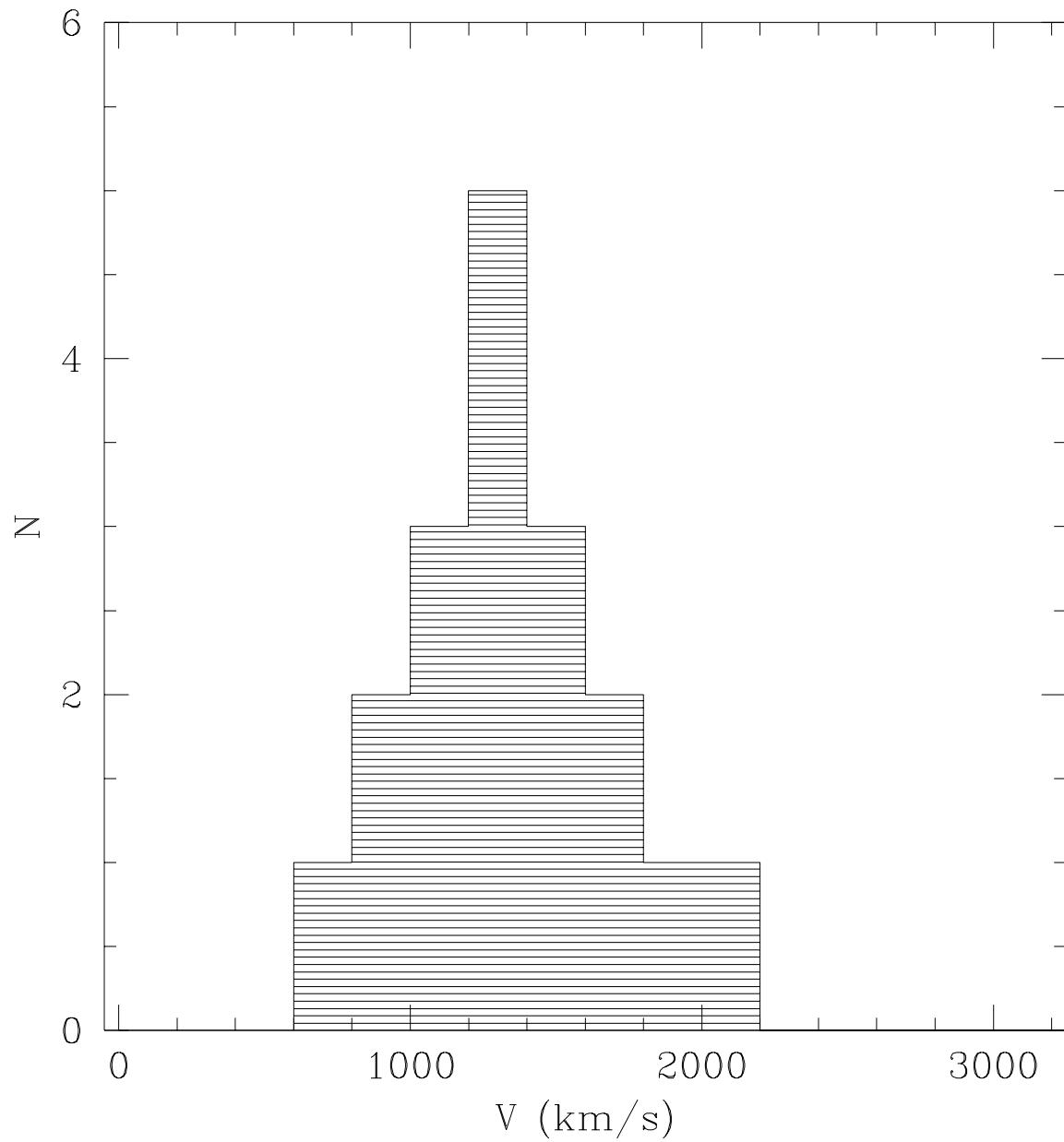


Fig. 4.— Velocity distribution for the 18 metal-rich globular clusters in NGC 1399.

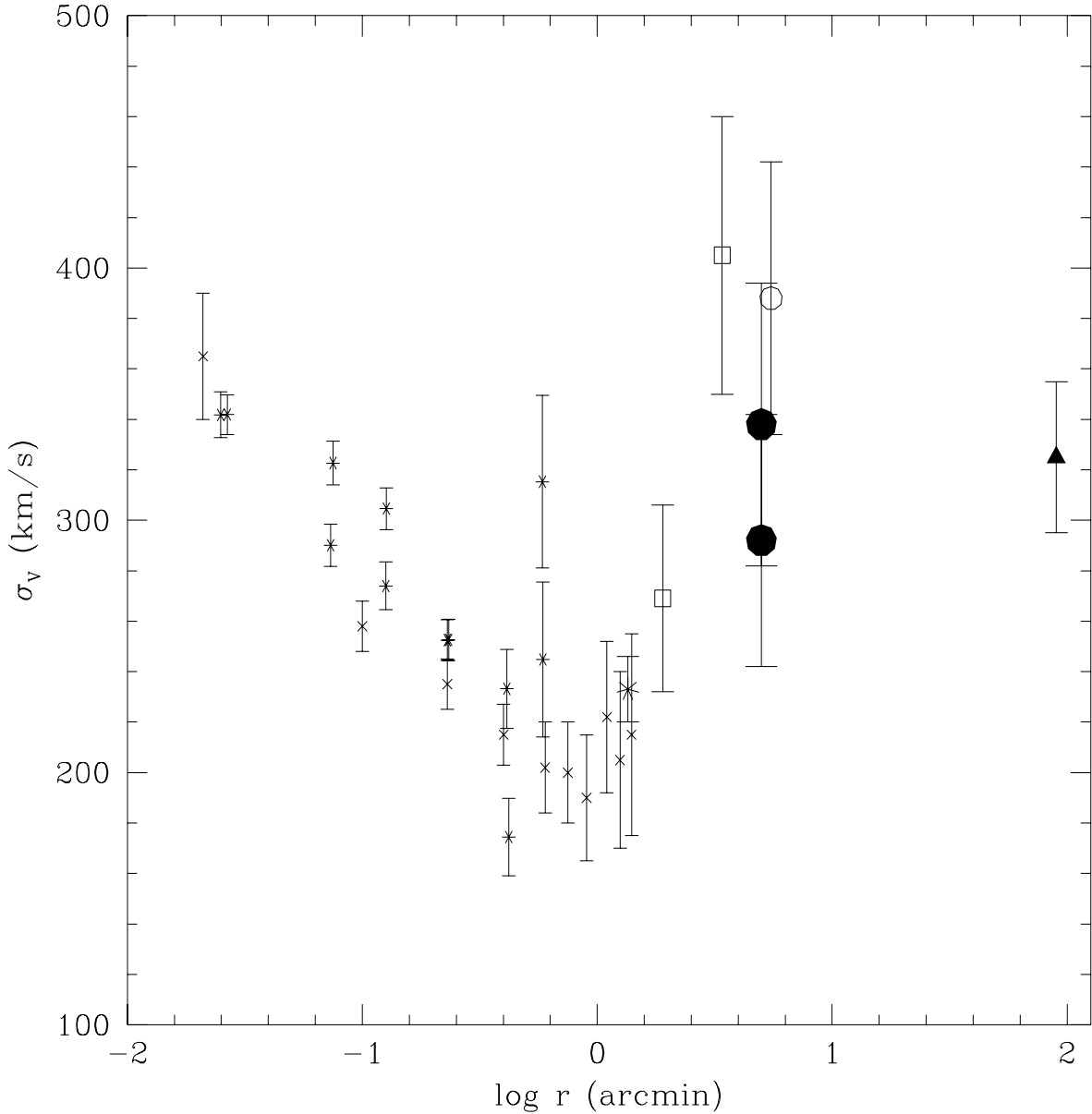


Fig. 5.— Radial dependence of the velocity dispersion in NGC 1399. The stars and crosses are from the integrated stellar light (Bicknell et al. 1989, Franx et al. 1989, Windsall & Freeman 1994), the open circle from the globular clusters of Grillmair et al. (1995), the squares from the planetary nebulae (Arnaboldi et al. 1994), the triangle from galaxies of the Fornax cluster (Ferguson 1989), and the filled circles from metal-rich globular clusters from this work (computed with and without the highest velocity cluster, see text).

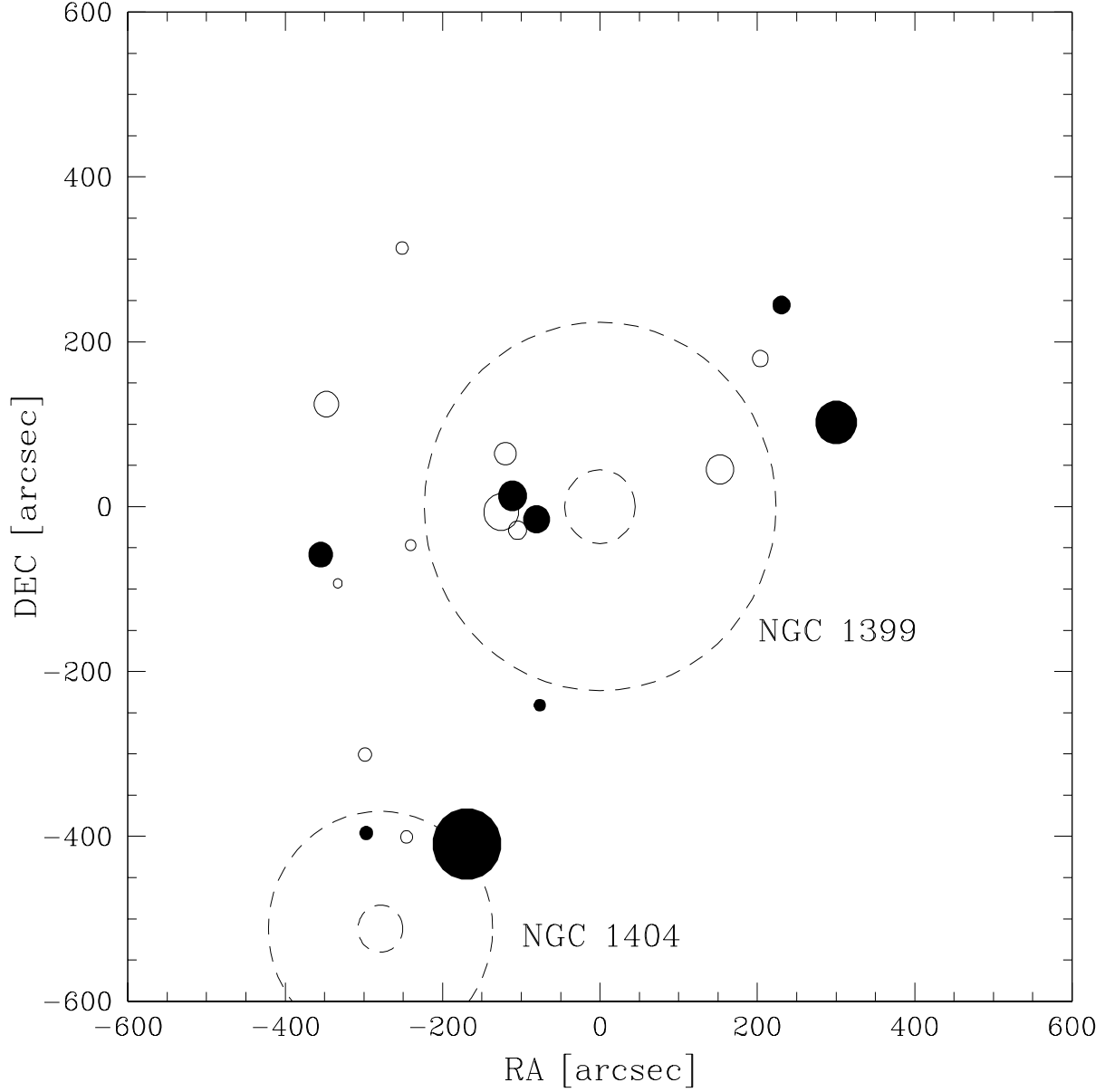


Fig. 6.— Spatial distribution of the confirmed globular cluster candidates with good radial velocities. The RA and DEC axes are in pixels, with North up and East to the left. The dashed circles show the location of the galaxies NGC 1399 and NGC 1404, respectively. The open and solid circles represent objects with $V < 1353$ and $V > 1353$ km s^{-1} , respectively, with their sizes scaling with the velocity difference to the mean $V = 1353$ km s^{-1} . Note that the data of field 1 (towards 1404) have twice the S/N than the rest, and that on field 2 and 4 we have only 3 and 4 globular clusters, respectively.